UPLINK CO-CHANNEL AND CO-POLAR INTERFERENCE STATISTICAL DISTRIBUTION BETWEEN ADJACENT BROADBAND SATELLITE NETWORKS

A. D. Panagopoulos

Mobile Radio Communications Laboratory
Division of Information Transmission Systems and
Materials Technology
School of Electrical and Computer Engineering
National Technical University of Athens
9 Iroon Polytechniou Street, Zografou GR 15780, Greece

Abstract—The reliable design of a satellite communications network, operating at Ku band and above, requires the exact evaluation of the interference effects on the availability and performance of both the uplink and downlink. In this paper, the case of Uplink Adjacent Satellite Network Interference is examined. We accurately calculate the deterioration of the uplink clear sky nominal adjacent satellite network Carrier-to-Interference threshold, due to spatial inhomogeneity of the propagation medium. At these frequency bands, rain attenuation is the dominant fading mechanism. Here we present an analytical physical model for the calculation of Interference Statistical Distribution between adjacent Broadband Satellite Networks operating at distances up to 500 km. We employ the unconditional bivariate lognormal distribution for the correlated rain fading satellite channels. Useful numerical results are presented for satellite networks located in different climatic regions and with various quality of service (QoS) assumptions.

1. INTRODUCTION

Commercial fixed satellite communication (satcom) networks already operate or will operate in the near future at frequencies above 10 GHz (Ku, Ka and V bands). At these frequency bands, rain attenuation is the dominant fading mechanism [1]. The reliable design of a satcom network requires the exact evaluation of the impact that has

interference on the availability of both the uplink and downlink [1].
A typical scenario of uplink interference is the following: co-channel
and co-polar adjacent satellite networks create mutual interference by
the return links of RCST (Return Channel Satellite Terminals) or
VSAT (Very Small Aperture Terminal) networks [1] (see Figure 1).
The rapid growth of satellite communications has led to congestion
on the geostationary orbit, where most of the commercial satcom
systems exist, (nowadays the satellites are separated by 2–3 degrees
in geostationary orbit). Furthermore, the employment of uplink
power control as uplink fade compensation technique [2] has become
very popular and standardized in the recent DVB-S and DVB-S2
networks [3]. Therefore an increase of an Earth station transmit power
to keep the flux density at the satellite input at a certain level, may
impair the operation of adjacent satellite networks. The problem
becomes more serious in urban areas due to the close existence of
Gateway and Earth terminals belonging to different satellite networks.
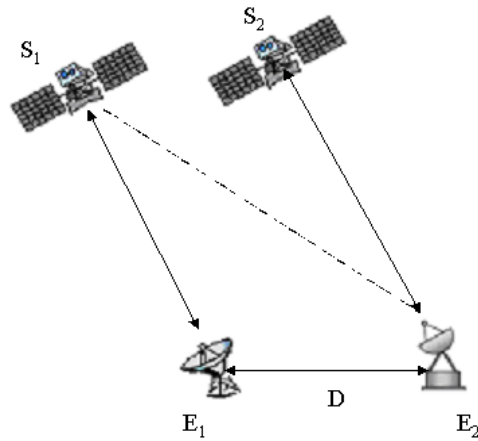
Figure 1. Configuration of the problem under consideration.

This paper investigates the aggravation of the uplink adjacent
satellite network interference due to spatial inhomogeneity of rainfall
medium. Rain attenuation exhibits stochastic behavior both in time
and space and can be generally considered as inhomogeneous [4–9].

The subject of the manuscript is the presentation of a physical
model for the calculation of the Interference Statistical Distribution
of the carrier-to-interference ratio (CIR) on the uplink taking into
account the Quality of Service's specification of the wanted uplink.
Under this assumption, we consider that the induced rain attenuation
of the wanted uplink is less than a maximum allowed preassigned

uplink rain fade margin M_u (dB). The interference effects are taken into account on the total outage time of the uplink under consideration.

The proposed method is based on an extended convective raincells model for the rainfall spatial structure and the assumption that both the point rainfall rate and the rain attenuation statistics follow the lognormal distribution [10]. We extend the correlation coefficient between rain attenuation variable in order to make the model valid for larger distances between the slant paths. The interference scenario is realistic considering the increase of the number of VSAT and DVB-RCS terminals in urban and rural areas and the increase of the penetration of interactive satellite services. The present predictive procedure is quite flexible, as it is oriented to be applicable to any location of the world.

The numerical results presented are focus on the analytical examination of the sensitivity of the carrier-to-interference ratio statistics with respect to the separation distance of the two interfering Earth terminals with a view to the optimum spectral coexistence of satellite communication networks in the same geographic area, the frequency of operation and the quality of service assumption for the uplink. Finally, design examples of various hypothetical satellite communication networks connected by Hellas Sat 2(39°E) located in regions with different climatic conditions are presented.

2. THE MODEL

The configuration of the problem is shown in Figure 1. The Earth terminal E_1 is assumed that belongs to a satellite communication network and is in communication with satellite S_1. Interference is caused by the return links of a second satellite communication network located adjacently in the same geographic area. The Earth terminal E_2 of this neighboring network is supposed to communicate with a second satellite S_2 in a very close orbit to S_1. Also, they are both assumed to operate at the same frequency and polarization as the return link of the satellite communication network under consideration.

The existing clear sky uplink interference scenario due to the antenna transponder side and satellite terminal lobes is mainly aggravated because of the existing differential rain attenuation along the wanted and interfering return links due to the spatial inhomogeneity of rainfall rate. More specifically, there may be periods of time, during which the rain induced attenuation A_1 (dB) on the wanted slant path would reduce the return signal sufficiently and allow interference from the return link of an adjacent Earth terminal which belongs to the collocated satcom network. We represent A_2 (dB) the

rain-induced attenuation on the interfering slant path. If the difference $A_1 - A_2$ may become large enough, so that the return link from the adjacent Earth terminal E_2 can cause significant interference on the uplink $E_1 S_1$.

The separation distance D of the two Earth-terminals is considered up to $500\,\text{km}$, which is small compared to the distance from the geostationary orbit, therefore the two slant paths are considered parallel. The elevation angles of the two slant paths are symbolized $\varphi_1\,(\text{deg})$ and $\varphi_2\,(\text{deg})$ respectively.

The Interference Statistical Distribution (ISD) is defined through:

$$ISD = P\left[CIR \leq CIR_{thr},\, r_M \leq A_1 \leq M_u\right] \qquad (1)$$

where $CIR\,(\text{dB})$ is the carrier-to-interference ratio level at the input of the satellite transponder under rain fades, $CIR_{th}\,(\text{dB})$ is the nonexceeded carrier-to-interference ratio level, while $r_M\,(\text{dB})$ is a threshold depending on the sensitivity of attenuation measurements [6] and is usually taken as $0.5\,\text{dB}$.

The main source of aggravation of UASN interference is the potentially existing differential rain attenuation of the two adjacent slant paths. As a result one can express the carrier-to-interference ratio under rain fades as:

$$CIR = (CIR)_{c.s.} - A_1 + A_2 \qquad (2)$$

In the above expression $(CIR)_{c.s.}$ is the carrier-to-interference power ratio at the transponder input during clear sky conditions depending on antenna diagrams, transmitted power, elevation angles and frequency of operation and ΔA is the differential rain attenuation factor.

The probability for the ISD in (1) can be calculated by simple straightforward algebra employing similar methodology as suggested in [11] for the calculation of conditional probability of differential rain attenuation statistics between two satellite converging links. Hence, that the Crane's simplified considerations [4, 12] have also been taken into consideration for the uniform vertical variation of the rainfall structure up to an effective rain height H that can be calculated from ITU-R rain height maps [13].

The above analysis assumes that both systems operate at perfect power control only compensating the free space loss factor and there is not power control scheme on rain attenuation part. If power control is assumed on rain attenuation with minimum and maximum power limits, the whole mathematical analysis that will include various limits of the random rain attenuation variables is different and this is a subject of future work.

Here we present the final formulas for the calculation of (1):

$$ISD = \frac{1}{2} \int\limits_{u_{1k}}^{u_{1p}} \frac{1}{\sqrt{2}} \cdot \exp\left(-\frac{u_1^2}{2}\right)\left(1 - \frac{1}{2} erfc\left(\frac{u_{1pk} - \rho_{n12}u_1}{\sqrt{2\left(1-\rho_{n12}^2\right)}}\right)\right) du_1 \tag{3}$$

where

$$u_{1p} = \frac{\ln M_u \cos\varphi_1 - \ln A_{m1}}{S_{a1}} \tag{4}$$

$$u_{1k} = \frac{\ln y_s - \ln A_{m1}}{S_{a1}} \tag{5}$$

$$u_0 = \frac{\ln r_M \cdot \cos\varphi_1 - \ln A_{m1}}{S_{a1}} \tag{6}$$

$$u_{1pk} = \frac{\ln\left([\exp(u_1 S_{a1}) + \ln A_{m1}]\frac{\cos\varphi_2}{\cos\varphi_1} - \left((CIR)_{c.s.} - CIR_{th}\right)\cos\varphi_2\right) - \ln A_{m2}}{S_{a2}} \tag{7}$$

and

$$y_s = \begin{cases} r_M \cdot \cos\varphi_1, & \left((CIR)_{c.s.} - CIR_{th}\right) < r_M \\ \left((CIR)_{c.s.} - CIR_{th}\right) \cdot \cos\varphi_1, & 0.5 \le \left((CIR)_{c.s.} - CIR_{th}\right) < M_u \\ M_u \cdot \cos\varphi_1, & M_u \le \left((CIR)_{c.s.} - CIR_{th}\right) \end{cases} \tag{8}$$

The derived expressions for the calculation of uplink interference statistical distribution are novel and can be easily calculated employing simple single integration algorithms. $A_{mi}, S_{ai} (i = 1,2)$ are the statistical parameters of the lognormally distributed rain induced attenuation on the satellite slant paths calculated properly using the methodology described in [11]. They are given in terms of $R_{mi}, S_{ri} (i = 1, 2)$ the lognormal parameters of point rainfall rate and are obtained through appropriate regression fitting analysis on ITU-R rainmaps [14]. Finally, the most important part of the ISD is the calculation of ρ_{n12}, the logarithmic correlation coefficient, which is given through the following formulas:

$$\rho_{n12}(D) = \begin{cases} \frac{1}{S_{a1}S_{a2}} \ln\left[\rho_{12}\sqrt{\left(e^{S_{a1}^2} - 1\right)\left(e^{S_{a2}^2} - 1\right)} + 1\right] & \text{for } D < 50\,\text{km} \\ 0.94e^{-\frac{D}{30}} + 0.06e^{-\left(\frac{D}{500}\right)^2} & \text{for } D \ge 50\,\text{km} \end{cases}, \tag{9}$$

The extension of correlation coefficient for separation distances over $D > 50$ km, has been proposed by Paraboni-Barbaliscia [15] and has been also employed for the prediction of large scale diversity schemes [16, 17].

ρ_{12} is the spatial correlation coefficient factor and can be calculated through:

$$\rho_{12} = \frac{H_2}{\sqrt{H_{11}H_{12}}} \tag{10}$$

$$H_2 = \int_0^{L_1} \int_0^{L_2} \rho_0\left(z, z'\right) \cdot dz \cdot dz' \tag{11}$$

$$H_{1i}\left(i = 1, 2\right) = 2L_i G \sinh^{-1}\left(\frac{L_i}{G}\right) + 2G^2 \left[1 - \sqrt{\left(\frac{L_i}{G}\right)^2 + 1}\right] \tag{12}$$

and

$$\rho_0(z, z') = \begin{cases} \dfrac{G}{\sqrt{G^2 + d^2\left(z, z'\right)}}, & d\left(z, z'\right) \leq D_r \\[2mm] \dfrac{G}{\sqrt{G^2 + D_r^2}}, & d\left(z, z'\right) \geq D_r \end{cases} \tag{13}$$

with (See geometrical details in Figure 2)

$$d\left(z, z'\right) = \sqrt{S^2 + (z' - K^2 - z)^2} \tag{14}$$
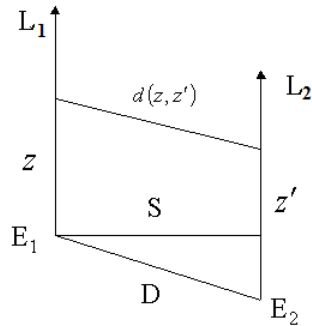
Figure 2. Slant paths projection. Calculation of spatial inhomogeneity factor.

and

$$K = \sqrt{D^2 - S^2} \tag{15}$$

$L_i\,(i = 1,2)$ are the effective slant path lengths and G is the characteristic parameter describing the inhomogeneity of the rainfall medium [11].

3. NUMERICAL RESULTS AND DISCUSSION

In the present section, the above suggested physical propagation model is employed for two hypothetical satellite VSAT networks located in different geographic regions in Europe (the first in Greece and the second in Italy) controlled by Hellas Sat 2 (39°E) geostationary satellite, and suffering from Uplink Adjacent Satellite Network Interference, due the spectral coexistence of the Earth-terminals.

In the uplink interference scenario in Greece, the wanted link is from an earth terminal located in Athens, GR, and the interfering uplink is coming from a terminal that is located in Volos, GR distant 312 km from Athens. The operational and geometrical parameters of the uplink interference scenario are tabulated in Table 1.

Table 1. Parameters of the uplink interference scenario in Greece.

Athens, GR	
Parameter	**Value**
R_m	0.03147
S_r	1.6877
G	1.5 Km
Elevation angle	43.4 degrees
(b) Volos, GR	
Parameter	**Value**
R_m	0.066364
S_r	1.4638
G	1.5 Km
Elevation angle	41.4 degrees

In Figures 3(a) and 3(b) for the interference scenario in Greece, we plot the ISD versus Carrier-to-Interference threshold for the two frequency bands Ku ($f = 14\,\text{GHz}$) and Ka ($30\,\text{GHz}$) band respectively.

We have considered two outage times (quality of service specifications) for the wanted link 0.01% and 0.001% that we can calculate the rain fade margins M_u. We have also considered $(CIR)_{c.s.} = 30\,\text{dB}$, a typical value for the modern satellite networks.
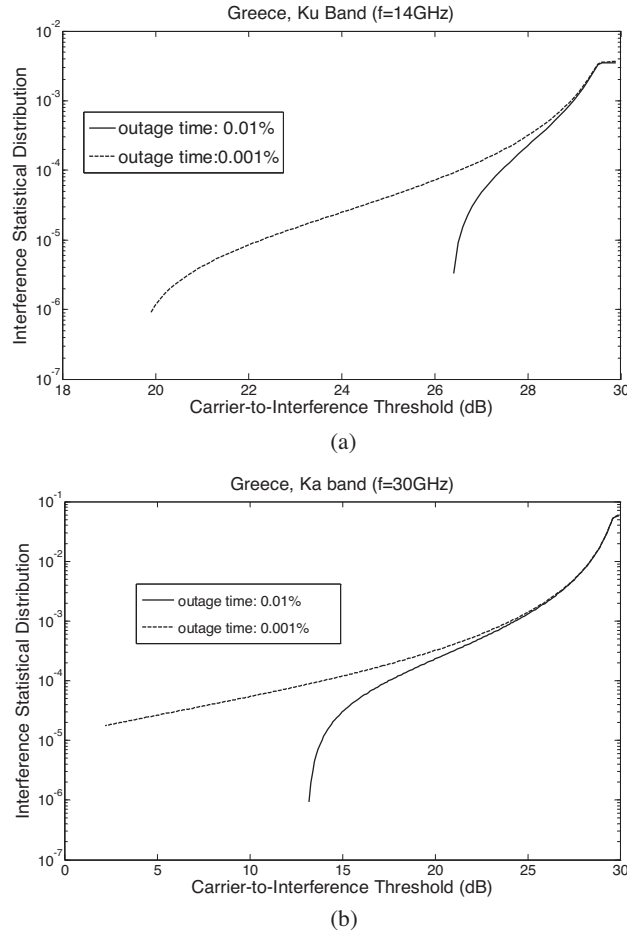
Figure 3. (a) Interference Statistical Distribution versus the *CIR* threshold level for an uplink interference scenario in Greece at Ku band uplink frequency for two outage time specifications of the wanted link. (b) The same but operating at Ka band uplink frequency.

In the uplink interference scenario in Italy, the wanted link is from an earth terminal located in Rome, IT, and the interfering uplink is coming from a terminal that is located in Naples, IT distant 189 km

from Rome. The operational and geometrical parameters of the uplink interference scenario are tabulated in Table 2. In Figures 4(a) and 4(b), the ISD is also drawn for the two frequency bands respectively, with the same clear sky carrier-to-interference ration.

Table 2. Parameters of the uplink interference scenario in Italy.

Rome, IT	
Parameter	**Value**
R_m	0.046819
S_r	1.6951
G	1.5 Km
Elevation angle	34.8 degrees
(b) Naples, IT	
Parameter	**Value**
R_m	0.039334
S_r	1.7494
G	1.5 Km
Elevation angle	36.7 degrees

From the Figures 3(a), 3(b), 4(a) and 4(b), we can observe that there is significant variation of carrier-to-interference ratio under rain fades due to the potential differential rain attenuation. The influence of the quality of service specifications on the predictive results of the ISD seems to be very important. The clear sky carrier-to-interference ratio, which is also a very important parameter in the whole analysis, remains constant and does not change with the variation of the separation distance, due to the fundamental assumption of the parallelism of the propagation paths. There is also an important impact of the climatic conditions on the predictive results. The aggravation of the interference is greater in the Italian scenario, due to the fact that the climatic conditions in Italian areas are heavier comparing to the Greek ones.

Moreover, in Figure 5, the predicted non-exceeded *CIR* levels, for given values of Interference Statistical Distribution and outage times, is plotted versus separation distances, for the Greek uplink interference scenario. The *CIR* threshold values are decreasing rapidly up to 50 km and almost remain constant up to 500 km. according to the assumption that $(CIR)_{c.s.}$ CIR remains constant and does not vary with the distance. More realistically, here we demonstrate the differential rain attenuation on parallel slant paths versus site separation distance. As the frequency increases, there is a deterioration of the achieved *CIR*
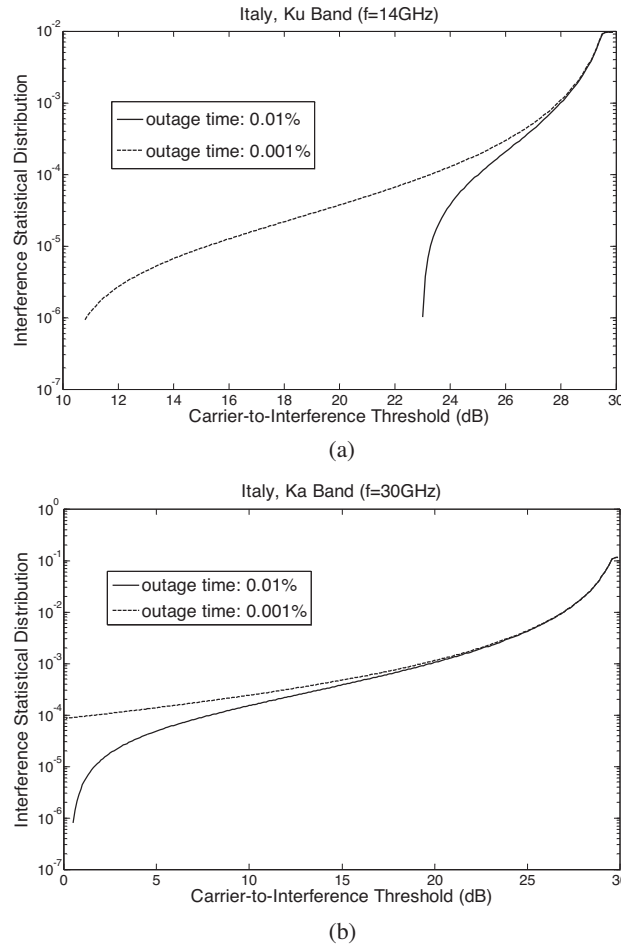
Figure 4. (a) Interference Statistical Distribution versus the *CIR* threshold level for an uplink interference scenario in Italy at Ku band uplink frequency for two outage time specifications of the wanted link. (b) The same but operating at Ka band uplink frequency.

threshold.

The same type of curves is presented in Figure 6 for the Italian scenario. The same conclusions regarding the dependence on separation distance may also be drawn. From both Figures 5 and 6, one can draw the conclusion that the aggravation of the uplink co-polar and co-channel interference is stronger on the satellite networks operating at Ka band and at heavier rain climatic regions.

Greece, Athens area, 0.01% outage time
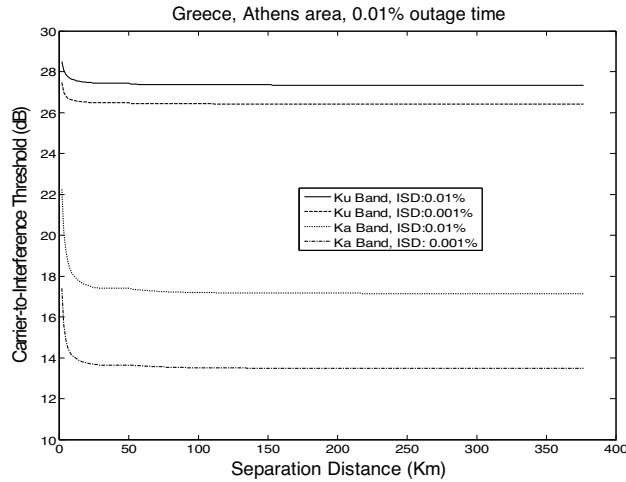
Figure 5. *CIR* nonexceeded threshold versus the separation distance D for the uplink interference scenario in Greece.

Italy, Rome Area, 0.1% outage time
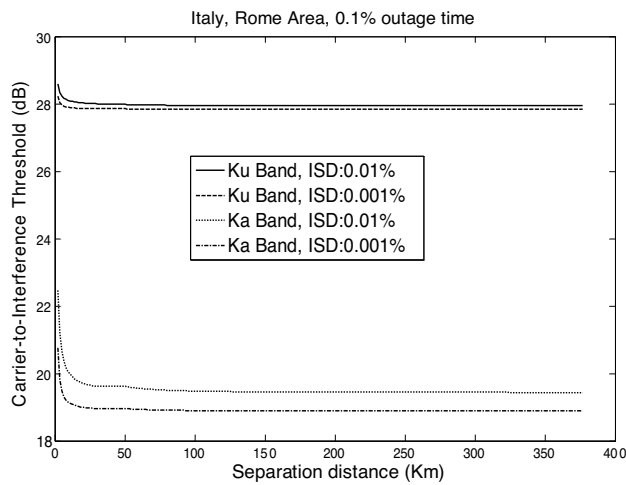
Figure 6. *CIR* nonexceeded threshold versus the separation distance D for the uplink interference scenario in Italy.

As a final remark, a thorough experimental verification of the proposed procedure is necessary in order to be able to validate the proposed close formulas expressions for the calculation of Interference Statistical Distribution.

4. CONCLUSIONS

For modern satellite communication networks using frequencies above 10 GHz, the uplink adjacent satellite network interference level is mainly aggravated due to the existing spatial inhomogeneity of the rainfall medium. The analysis presented in this paper concerns the prediction of the carrier-to-interference ratio statistics of an uplink interfered by another uplink belonging to an adjacent satellite network for distances up to 500 km. The main conclusion of the analysis is that the separation distance of the interfering Earth-station from the wanted Earth-terminal does not aggravate more the degradation of the carrier-to-interference ratio on the uplink.

REFERENCES

1. Panagopoulos, A. D., P.-D. M. Arapoglou, and P. G. Cottis, "Satellite communications at Ku, Ka, and V bands: Propagation impairments and mitigation techniques," *IEEE Commun. Surveys and Tutorials*, Third Quarter, 2004.

2. Castanet, L., A. Bolea-Alamañac, and M. Bousquet, "Interference and fade mitigation techniques for Ka and Q/V band satellite communication systems," *COST 272-280 International Workshop on Satellite Communications from Fade Mitigation to Service Provision*, Noordwijk, The Netherlands, May 2003.

3. Morello, A. and V. Mignone, "DVB-S2: The second generation standard for satellite broad-band services," *Proceedings of the IEEE*, Vol. 94, No. 1, 210–227, Jan. 2006.

4. Crane, R. K., *Electromagnetic Wave Propagation through Rain*, Wiley Series in Remote Sensing, 1996.

5. Mandeep, J. S., "Rain attenuation predictions at Ku-band in South East Asia countries," *Progress In Electromagnetics Research*, PIER 76, 65–74, 2007.

6. Mandeep, J. S., "Equatorial rainfall measurement on Ku-band satellite communication downlink," *Progress In Electromagnetics Research*, PIER 76, 195–200, 2007.

7. Chen, K.-S. and C.-Y. Chu, "A propagation study of the 28 GHz LMDS system performance with M-QAM modulations under rain fading," *Progress In Electromagnetics Research*, PIER 68, 35–51, 2007.

8. Ojo, J. S., M. O. Ajewole, and S. K. Sarkar, "Rain rate and rain attenuation prediction for satellite communication in Ku and Ka

bands over Nigeria," *Progress In Electromagnetics Research B*, Vol. 5, 207–223, 2008.

9. Ojo, J. S. and C. I. Joseph-Ojo, "An estimate of interference effect on horizontally polarized signal transmission in the tropical locations: A comparison of rain-cell models," *Progress In Electromagnetics Research C*, Vol. 3, 67–79, 2008.

10. Drougas, A. E., A. D. Panagopoulos, and P. G. Cottis, "Stochastic verification of the first-order Markovian assumption of rain attenuation for satellite channel dynamic modeling," *IEEE Communication Letters*, Vol. 12, No. 9, 663–665, Sep. 2008.

11. Kanellopoulos, J. D., A. D. Panagopoulos, and S. N. Livieratos, "A comparison of copolar and cochannel satellite interference prediction models with experimental results at 11.6 and 20 GHz," *Int. Jour. of Sat. Commun.*, Vol. 18, 107–120, 2000.

12. Crane, R. K., *Propagation Handbook for Wireless Communication System Design*, CRC Press LLC, 2003.

13. ITU-R P.839-3, "Rain height model for prediction methods," Geneva, 2003.

14. ITU-R P.837-4, "Characteristics of precipitation for propagation modeling," 2003.

15. Barbaliscia, F., G. Ravaioli, and A. Paraboni, "Characteristics of the spatial statistical dependence of rainfall rate over large areas," *IEEE Trans. on Ant. and Prop.*, Vol. 40, No. 1, 8–12, 1992.

16. Panagopoulos, A. D., P.-D. M. Arapoglou, A. D. Panagopoulos, G. E. Chatzarakis, J. D. Kanellopoulos, and P. G. Cottis, "Unbalanced large scale multiple site diversity performance in satellite communication networks," *XXVIIIth URSI General Assembly*, 2005.

17. Luglio, M., R. Mancini, C. Riva, A. Paraboni, and F. Barbaliscia, "Large-scale site diversity for satellite communication networks," *International Journal of Satellite Communications*, Vol. 20, No. 4, 251–260, July–August 2002.